Drops sliding along an inclined plane: Experiments versus 3D hydrodynamic model

A. Daerr*, N. Le Grand* , L. Limat* and H. A. Stone**

*Laboratoire de Physique et Mécanique des Milieux Hétérogènes, UMR 7636 of CNRS, ESPCI, 10 rue Vauquelin, 75231 Paris Cedex 05, France

** Division of Engineering and Applied Sciences, Harvard University, Cambridge MA 02138, USA

Abstract

We present recent experiments on drops sliding along an inclined plane in situation of partial wetting. Above a critical capillary number the contact line edging the drops becomes singular at the drop rear: a "corner" developes, where the contact line exhibits an angulous shape. Views taken from above and from the side show that this occurs when a non-zero critical dynamic angle is reached at the drop rear, the interface assuming a conical shape. This conical shape is recovered by seeking a 3D similarity solution of the flow near the corner tip in the lubrication approximation. This model reproduces accurately the correlations between two characteristic angles of the cone.

1. Introduction

When a tape or a plate is pulled out of a bath at constant speed, in situation of partial wetting, a triangular film edged by a sawtooth contact line is observed insteed of the expected Landau film driven by the tape motion (Burley 1975, Blake 1979). A similar phenomenon has been recently identified on drops sliding along an inclined plane (Podgorski 2001). When the capillary number $Ca = \eta U / \gamma$ (U drop velocity, η viscosity, γ surface tension) exceeds a critical value, the initially rounded perimeter of the drop exhibits a singularity at the drop rear (see Figure 2-c). A "corner" developes where two contact lines are crossing each other separated of an angle 2ϕ. This "corner opening angle" is linked to Ca by a scaling of the kind $\sin\phi \propto 1/Ca$ that is qualitatively explained as follows. When Ca is progressively increased, the dynamic contact angle reduces at the drop rear until reaching zero, value for which a Landau film should be deposited on the solid. Instead of this, the contact line becomes tilted in order to keep the effective capillary number $Ca \sin\phi$ defined in a direction normal to contact line locked to the critical value, the system lying just at the transition. Recent preliminar observations (Limat 2002) and an approximate model of the flow in the corner (Stone 2001) are inconsistent with the idea of a vanishing contact line at the drop rear. We therefore present here more accurate visualizations of such drops (Daerr 2003) and more rigorous calculations of the flow including 3D effects (Limat 2003).

2. Experiments

Trains of millimetric silicon oil drops (volume 6 mm^3) are poured at the top of an inclined glass plate coated with fluoropolymers (3M FC725 compound). Varying the plate inclination allows us to change at will the drop velocity. We used three diferent oils of respective viscosities η=10, 100 and 1000 cP, mass density of order 0.95 g/cm^3, and surface tension of order 20 mN/m. By using a mirror and an appropriate optical method we were able to visualize the drop from both the top and the side as dark shapes on a clear background. Examples are displayed on Figure 1. At low velocities (case a), the drops are rounded and the side view allows us to measure quite accurately the dynamic advancing and receding contact angles θ_a and θ_r. At higher drop velocity, a corner developes (cases b and c). As one can judge from the side view, the structure of the interface becomes conical at the drop rear, the cone being parametrized by the angles ϕ (corner opening angle) and Ω (slope of the interface viewed from the side). At even higher velocities, a cusp is observed instead of the corner (case d), and a pearling transition with droplet depositions at the cusp tip (case e).

We have plotted on Figure 2 the evolution versus Ca of the angles θ_a, θ_r (measured only on rounded drops), ϕ, Ω for the 10 cP silicon oil. The θ_a and θ_r measurements are well described by a Cox-Voïnov law:

$$\theta_{a/r}^3 = \theta_S^3 \pm 9\ln(b/a)Ca \qquad (1)$$

with $\theta_S = 44°$ for the receding contact angle and $\theta_S = 51°$ for the advancing contact angle. Both cases have nearly the same logarithmic parameter value 9Log(b/a)=130, a remarkable fact that we found for the three used oils.

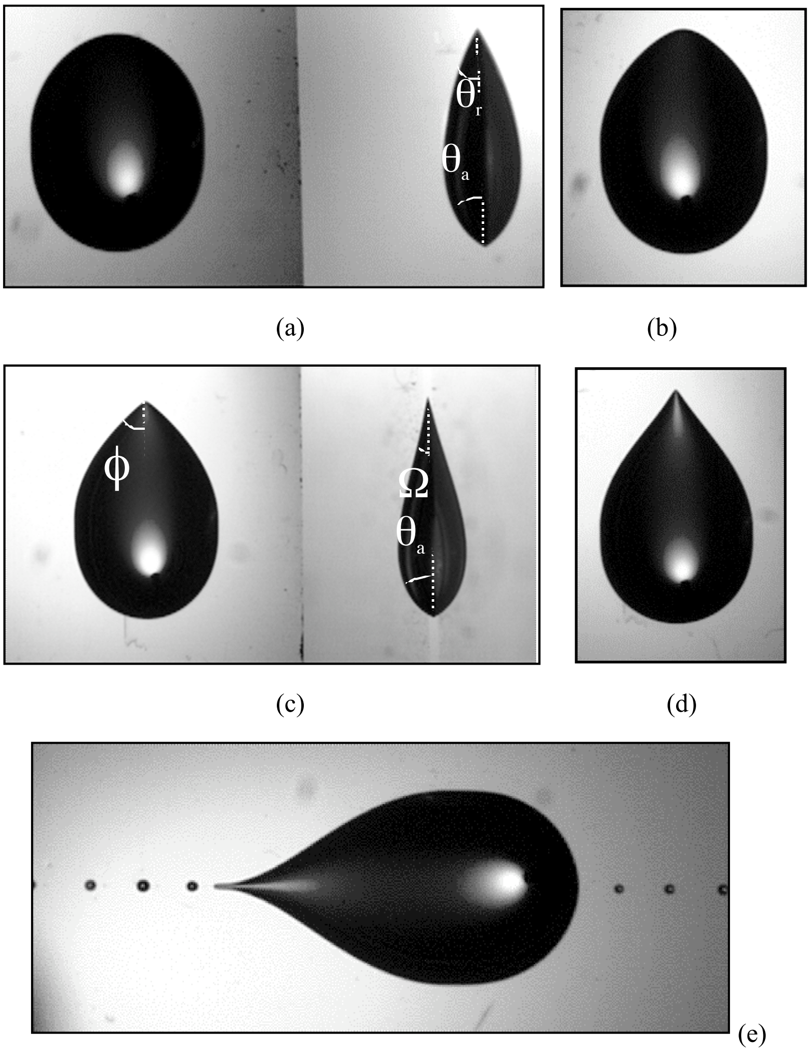

Figure 1: Drops sliding (from top to bottom except in case e) on an inclined glass plate for increasing velocities: (a) rounded drops, (b) limit of corner formation, (c) cornered drops, (d) cusped drop, (e) pearling drop. In case (a) and (c) the picture taken from above (on the left) is presented with a picture taken from the side (on the right), itself doubled by a reflection on the glass.

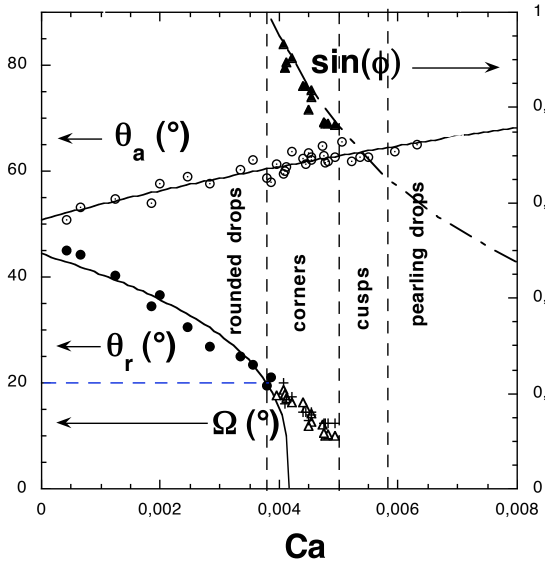

Figure 2: Evolution versus Ca of θ_a (o), θ_r (●), ϕ (▲) and Ω (△), deduced from the pictures for a 10 cP silicon oil. (+): Ω predictions from Equation (6).

This is a strong indication suggesting that the hydrodynamic model is well adapted to describe our system.

In the corner regime, the surprise here, that confirms in fact our previous observations (Limat 2002) is that the corner appears for a non-zero critical value of the dynamic contact angle at the drop rear, of order here θ_c=20°. Let us note however that the critical capillary number of the corner formation remains close to the value at which θ_r touches down. In this sense, the initial qualitative argument is not so far from the truth. Still in the corner regime, ϕ is well described by a $1/Ca$ law, which suggests that instead of remaining locked on $\theta_r(Ca \sin\phi)=0$, the system is locked on θ_r $(Ca \sin\phi)=\theta_c$, which implies from equation (1) that:

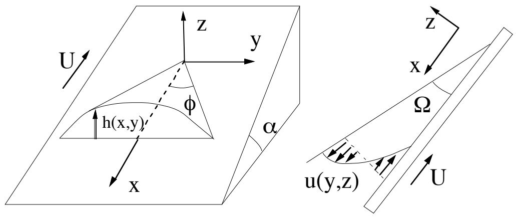

Figure 3: Model suggested in the drop framework (ascending plate).

$$\sin\phi \approx \frac{\theta_s^3 - \theta_c^3}{9Log(b/a)}\frac{1}{Ca} \qquad (2)$$

with again θ_S=*46°=0.80 rd* , θ_c=*17°=0.30 rd* and *9*Log(*b/a*)=*130.*

Finally, let us also mention that , still in the corner regime, *Ω* is in continuity with the trace of *θ(Ca)* in the oval regime. Though rather intuitive, this result is not obvious since in this conical structure the contact angle (defined normaly to contact line) does not coincide with *Ω*. Imaginating the detail of the involved geometry still remains a puzzling problem.

3. 3D Model of the corner.

The qualitative ideas used above are reasonable but, up to now, there is no theoretical proof of the fact that $Ca\sin\phi$ is the relevant capillary number, i.e. that all the contact line properties are governed in some sense by the velocity component normal to contact line. Also, a rigorous model of the flow near the corner is still lacking, despite the simplified approach provided in our previous papers (Stone 2001, Limat 2002). We provide here a brief account of a more rigorous approach published very recently (Limat 2003). Let us mention that another model has been proposed by another group but based upon different physical assumptions (Benamar 2001).

In a framework moving with the liquid surface, i.e. in which the free surface is static, the plate is moving along the Ox axis of Figure 3 with a velocity –U. This induces a liquid flux towards x<0 that is balanced by a flux in the opposite direction induced by the pressure singularity at the corner tip. The situation is in turn complicated by the existence of a component of velocity directed along Oy. In the lubrication approximation (low angle limit with negligible inertia), the balance of liquid reads:

$$3Ca\frac{\partial h}{\partial x} = \nabla.\left[h^3\nabla(\Delta h)\right] \tag{3}$$

where h(x,y) denotes the local thickness of liquid and $\nabla = (\partial_x, \partial_y)$. Very near the tip of the corner, one can seek for similarity solutions of the kind $h(x,y) = Ca^{1/3}H(\varsigma = y/x)$. This leads to an ordinary differential equation

$$\begin{aligned}&(1+\varsigma^2)^2(H^3H_{\varsigma\varsigma\varsigma})_\varsigma + 3\varsigma(1+\varsigma^2)(H^3H_{\varsigma\varsigma})_\varsigma\\&+2\varsigma(1+\varsigma^2)H^3H_{\varsigma\varsigma\varsigma} + (1+3\varsigma^2)H^3H_{\varsigma\varsigma} = 3(H-\varsigma H_\varsigma)\end{aligned} \tag{4}$$

that must be completed with a zero flux condition across the cross-section of the cone, the flux integrated on a cross section reading:

$$J_x = 2\int_0^{\zeta x} j_x dy = \frac{2}{3}\frac{\gamma}{\eta}Ca^{4/3}x^2\int_0^{\zeta} K(\zeta')H^3(\zeta')d\zeta'$$

with: (5)

$$K(\zeta) = \frac{d}{d\varsigma}\left[\zeta(1+\zeta^2)\frac{d^2H}{d\zeta^2}\right] + \frac{3}{H^2}$$

The numerical simulation of the solutions of this problem are reproduced on Figure 4 and compared to a previous approach neglecting the Oy velocity of the flow ("planar flow approximate"), and to an even simpler parabolic approximate of the cross-section discussed in the same reference (Stone 2001). As one can judge from this figure, the 3D nature of the flow does not change too much the situation with respect to the planar model, at least near the center of the cone cross section. On the same Figure we have reproduced the predictions of this approach for the relationship linking the two angles ϕ and Ω across the quantity $H(0)=H_0=Ca^{-1/3}\tan\Omega$. Remarkably, both the 3D and planar flow models are quite well described by the result of the parabolic approximate that gives:

$$\tan^3\Omega \approx \frac{3}{2}H_0^3 = \frac{3}{2}Ca\tan^2\phi \tag{6}$$

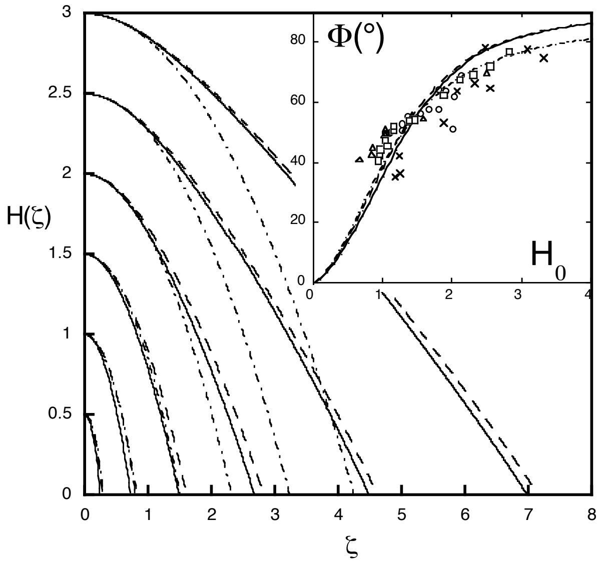

Figure 4: Calculated profiles of the cone cross section, the free surface being given by $h=Ca^{1/3}xH(\zeta=y/x)$. Insert : Relationship linking the opening corner angle ϕ to $H_0=Ca^{-1/3}$. Continuous lines : full 3D solution. Dashed lines: planar flow approximation . Dash-dotted lines: parabolic approximation for the cross sectional shape. (✕): experimental values deduced from (Limat 2002) obtained with silicon oil drops sliding on fluoropolymers, γ =20 mN m^{-1}, η =20 cP. Open symbols: measurements from (Daerr 2003) discussed in section 2: (○) η=10 cP, (△) 100 cP, and (□) 1000 cP, with again γ=20 mN m^{-1}.

Experimental data extracted from our measurements for the three oils used are compared to this law that seems to work remarkably well. Just as for the mobility law of Equation 1, it seems that despite its well known limitations, the classical hydrodynamic model works very well in our situation.

Finally we have checked how behaves our solutions very near each contact line. We found that the singularity of thickness reads:

$$h \approx (9Ca\sin\phi)^{1/3}\,\xi(-Log|\xi|)^{1/3} \tag{7}$$

where $\xi = x\sin\phi - y\cos\phi$ designates the coordinate normal to the contact line. This expression is consistent with the idea that – at least qualitatively – the contact line behaves following the Cox-Voïnov model, after replacing the capillary number with the effective value $Ca\sin\phi$ All these findings are consistent with the qualitative ideas discussed in the experimental part, that, perhaps for the first time receive the begining of a justification starting from hydrodynamics.

4. References

Burley, R. and Kennedy, B., 1976, An experimental study of air entrainment at a solid/liquid/gas interface, *Chem. Eng. Sci.* **31**, 901-911

Blake, T.D. and Ruschak, K.J., 1979, A maximal speed of wetting, *Nature* **282**, 489-491

Podgorski T., Flesselles J.-M. and Limat L., 2001, Corners, cusps and pearls in running drops, *Phys. Rev. Lett.* **87**, 036102-036105.

Limat L., Podgorski T., Flesselles J.-M., Fermigier M., Moal S., Stone H. A., Wilson S.K., Andreotti B., 2002, Shape of drops sliding down an inclined surface, *Advances in Coating Processes,* edited by J.-M. Buchlin et al, pp.53-58, Von Karman Institute Press, Bruxelles.

Stone H.A., Limat L., Wilson S.K., Flesselles J.-M., and Podgorski T., 2001, Corner singularity of a contact line moving on a solid surface, *C.R. Physique* **3,** 103-110.

Daerr A. Le Grand N. and Limat L., 2003, Drops sliding along an inclined plane, preprint.

Limat L. and Stone H. A., 2003, Three-dimensional lubrication model of a contact line corner singularity, *Europhysics*, to appear.

Ben Amar M. , Cummings L. , and Pomeau Y. 2001, Singular points on a receding contact line, *C. R. Acad. Sci. (Paris)* **329**, II-b, 277-282.